ENERGY REDUCTION IN MECHANICAL PULPING

APRIL 2018

THE UNIVERSITY OF BRITISH COLUMBIA

WELCOME MESSAGE

Dear partners in the Energy Reduction in Mechanical Pulping research program,

The UBC Bio-Products Institute (BPI), which will eventually encompass the Pulp and Paper Centre and its research initiatives, continues its successful work on securing funding and ramping up efforts to recruit and build infrastructure. I am pleased to report that through the $3 million UBC President's Excellence Chair in forest bio-products, the hiring team is in the process of a recruiting decision. BPI's application for a Canadian Excellence Research Chair award, which will provide $20 million from the federal government and UBC to bring a world-leading researcher to UBC and the BPI has been approved, and recruitment is now underway.

Following the BPI's successful proposals to the Canadian Foundation for Innovation (CFI) funding for $11.6 million for infrastructure related to synthetic biology-enabled materials for high performance biocomposites (BiMat), as well as BCKDRF funding for a $6 million proposal for a Biofuels Research and Innovation Centre (BRIC), the procurement process is underway. This funding will bring cutting edge research tools and instrumentation to UBC, including tools for advanced pulp and paper characterization, such as micro-computed tomography (micro-CT) X-ray scanning equipment valued at $2 million — powerful technology for our future research initiatives.

It is also exciting to share with you that as the result of a strong Letter of Intent, BPI's BioInnovative Renewables Network (BIRNet) with UBC as the lead university, has been invited to submit a full proposal to the $51.2 million grant application ($20.9 million NSERC component) to NSERC's Networks of Centres of Excellence (NCE) program competition. This program is a highly competitive process with only the top applications selected to move to this final stage. The NCE program helps expand global knowledge in strategic areas and enables the creation and implementation of multifaceted solutions to specific social and economic challenges in Canada.

Since our last newsletter, we held a successful ERMP Steering Committee meeting in November at UBC where we reviewed research project progress, and discussed ongoing energy reduction initiatives and challenges among our partners. While we will not be holding a meeting in conjunction with the PACWest conference this year, we look forward to meeting with all of our partners at our next Steering Committee meeting in the fall of 2018 — please watch for a "Save the Date" in the new few months. We also held the latest Andritz trials in December 2017, which we summarize on page 26, and will present at the next Steering Committee meeting.

We also have several personnel updates. Program Manager Meaghan Miller has begun a 1-year parental leave and will return in March 2019. We are working on hiring a replacement, who will focus on the ongoing development of a new NSERC CRD proposal, the initial draft for which we continue to seek comments and commitments. Postdoctoral Fellow Zhaoyang Yuan has left UBC for Michigan State University for a position in Biochemistry and Molecular Biology, where he will focus on improving and optimizing the operation process to produce biofuels and co-products from biomass. Several ERMP students including Jorge Rubiano, Hui Tian and Taraneh Kordi are working towards graduation in the next few months. I invite you to read more about our project updates and publications in the following pages.

Finally, I am very pleased to share that I was appointed the new Dean of the Faculty of Applied Science at UBC, a 5-year term that began on March 1, 2018. This role will enable me to continue my dedicated efforts to UBC Applied Science, through research and funding initiatives and goals such as increasing engineering education throughout British Columbia. My role as Dean includes dedicated research time, and I remain committed to our continued success through university–industry research partnerships.

Sincerely,

James Olson, PhD, P.Eng, FCAE
Dean of the Faculty Applied Science and Professor of Mechanical Engineering, UBC
Principal Investigator, ERMP Research Program

CONTRIBUTORS

Matthias Aigner
Bryan Bohn
Jose Gabriel Dimayacyac
Reza Harirforoush
Taraneh Kordi
Meaghan Miller
James Olson
Jorge Rubiano
Reanna Seifert
Bahar Soltanmohammadi
Hui Tian
Vanessa Van Aert
Miguel Villalba

PRODUCTION EDITOR and DESIGNER
Chitra Arcot

MAILING ADDRESS
Pulp and Paper Centre
2385 East Mall
Vancouver, BC V6T 1Z4

EMAIL
Communications Coordinator
Chitra.Arcot@ubc.ca
Phone: 604.827.2117

PRINTER
Minuteman Press

CONTENTS

RESEARCH UPDATES

PROGRAM UPDATES

CONTACTS

ON THE COVER

ERMP researcher Miguel and research technician Reanna process wood chip samples through brass sieves of different screen sizes. The largest screen (right) has 0.5 inch holes. The two stacked sieves containing wood chip samples have screens of 0.25 and 0.12 inches. The sieved samples are then treated for compression and enzymatic hydrolysis.
Photo credit: Chitra Arcot

MIGUEL VILLALBA

PROJECT 1.1 COMPRESSION SCREW FEED OPTIMIZATION AND ENERGY SAVINGS IN HC REFINING

In the thermomechanical pulping process, compression is used as a method to improve the chemical uptake properties of wood chips. A combination of compression and chemical impregnation prior to refining leads to a reduction of energy requirements in the subsequent refining stages (Nelsson et al. 2012; Gorski et al. 2010). The use of enzymes as a chemical agent in impregnation positively influences energy reduction and improves pulp properties (Hart et al. 2009). This project focuses on understanding the effects of screw press operating conditions (i.e. screw speed, power input and geometries) on wood chip morphology that relate to its chemical uptake ability. We then focused our efforts on developing a simple screw press model that would characterize the operation of a modular screw press device for wood chips. Research literature contains multiple studies that characterize changes in chip morphology and liquid uptake, but few exist that asses the effect of compression on enzyme accessibility. Therefore, we aim to understand the effect compression has on the accessibility of enzymes on wood chips.

Enzyme accessibility study

The experimental part of our research involved compressing wood chips to different degrees and impregnating them with enzymes at ideal conditions (Figure 1). We assessed enzyme hydrolysis by using the sugar quantification method. Sugars are quantified before compression and after enzyme impregnation by methods outlined by the National Renewable Energy Laboratories (NREL). We performed compositional analysis of the solid biomass according to the standard Klason Lignin protocol (Sluiter et al. 2012).

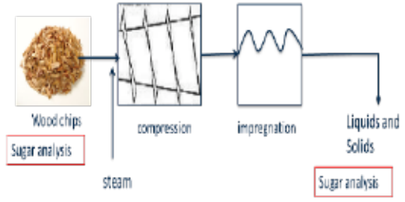

Figure 1: Experimental layout.

Figure 2: Kraft pulp, BCTMP, SPF sawdust and SPF wood chips (left to right).

Enzyme activity is highly dependent on available surface area of cellulose (in the case of cellulases) and biomass composition, keeping temperature and pH constant and at their optimum conditions. We performed an enzyme accessibility study for biomass of different compositions and morphologies as follows: ground Kraft pulp, and Bleached Chemi-ThermoMechanical Pulp (BCTMP), spruce-pine-fir (SPF) sawdust and wood chips (Figure 2).

The samples were subjected to enzyme hydrolysis in an incubator shaker rotating at 120 rpm at optimal enzyme conditions (temperature 50oC, and pH 4.8). The enzyme used, provided by AB Enzymes, was mainly composed of exoglucanase at a high dosage of 100 mg/g ODW. Samples were placed in flasks with a mixture of sodium acetate buffer and enzyme. Liquid samples were extracted over time for high performance liquid chromatograph (HPLC) analysis. Results (Figure 3) confirmed that the enzyme activity was affected by the composition and morphology of the samples.

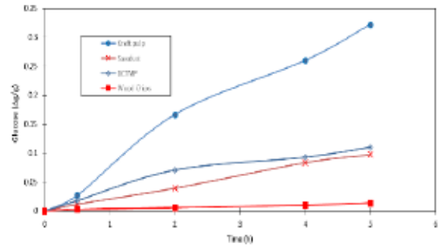

Figure 3: Normalized sugar released over time. Here, Δg/g represents released grams of glucose in the liquor over the initial glucose amount of the solid sample. Samples were treated with cellulase enzyme at optimal conditions.

Figure 4: Left (a) Chip Juicer device. 4(b) Visual comparison between control (centre), and 4(c) 4:1 compressed chips (right). Visually speaking, there seems to be just a small change in structure compared to that achieved by an Impressafiner.

PROJECT 1.1

Kraft pulp has high glucose and negligible lignin content (87% and >1%, respectively). SPF wood has lower glucose content and higher lignin content (40% and 33%, respectively). BCTMP values lie in between the Kraft and SPF wood. Differences in composition account for the higher enzyme activity between the pulps, while mass transfer justifies the difference between the sawdust and chips. The enzymatic activity attained with the sawdust should be the highest in comparison to any compressive pretreatment by screw feeding of wood chips.

Chip juicer trial

Chip compression trials conducted with FPInnovations took place in Pointe Claire, Quebec using a chip juicer (Figure 4), a piston-like device. The wood chips were pre-steamed for 20 minutes. The chips (~200 g) were compressed at different compression ratios (i.e. 2:1, 3:1 and 4:1). For each test, the retention time required to achieve a compression ratio was recorded to estimate power consumption. The compressed chips were then subjected to enzyme treatment to quantify sugar release.

The results (Figure 5) from this trial show slightly greater sugar release as compression ratio increases. We observed that the rate of hydrolysis for each case is more rapid in the first 45 minutes and becomes almost constant for all compression ratios.

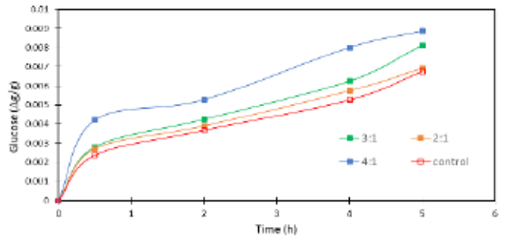

Figure 5: Normalized sugar released (Δg/g) over time for wood chips compressed at different compression ratios. Wood chips were treated with cellulase enzyme at optimal conditions.

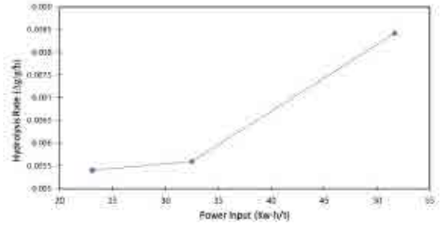

Figure 6: Hydrolysis rate (Δg/g/h) as function of power consumption of the chip juicer (kW-h/t).

This could indicate that the enzyme has penetrated and then diffused into the chip when the sugar release starts to plateau. Regardless, the initial hydrolysis rate increases with compression ratio and power consumption (Figure 6).

Future research

We plan on conducting more trials with a mechanical testing system (MTS) compression device. Different compression ratios and compression rates will be tested simulating screw feeder operations. The objective is to achieve higher defibrillation of wood chips than what the chip juicer achieved. Future screw feeder trials are to be planned in the summer. Enzyme accessibility and screw feeder operation will be evaluated.

References

Gorski, Dmitri, Jan Hill, Per Engstrand, and Lars Johansson. 2010. "Review: Reduction of Energy Consumption in TMP Refining through Mechanical Pre-Treatment of Wood Chips." *Nordic Pulp and Paper Research Journal* 25 (2):156–61.

Hart, Peter W., Darrell M. Waite, Luc Thibault, John Tomashek, Marie Eve Rousseau, Christopher Hill, and Marc J. Sabourin. 2009. "Selective Enzyme Impregnation of Chips to Reduce Specific Refining Energy in Alkaline Peroxide Mechanical Pulping." *Holzforschung*. https://doi.org/10.1515/HF.2009.065.

Nelsson, Erik;, Sandberg; Christer, Lars; Hilden, and Geoffrey Daniel. 2012. "Pressurised Compressive Chip Pre-Treatment of Norway Spruce with a Mill Scale Impressafiner." *Nordic Pulp and Paper Research Journal* 27 (1):056–062. https://doi.org/10.3183/NPPRJ-2012-27-01-p056-062.

Sluiter, A., B. Hames, R. Ruiz, C. Scarlata, J. Sluiter, D. Templeton, and D. Crocker. 2012. "NREL/TP-510-42618 Analytical Procedure - Determination of Structural Carbohydrates and Lignin in Biomass." *Laboratory Analytical Procedure*. https://doi.org/NREL/TP-510-42618.

JOSE GABRIEL DIMAYACYAC

1.3 - OPTIMIZATION OF CHEMICAL CHARGE DISTRIBUTION THROUGHOUT THE PROCESS

Growing demands for paper products can be met through producing high yield thermomechanical pulps. The disadvantage of thermomechanical pulp (TMP) is that its production consumes a large amount of electrical energy. A promising strategy to overcome this drawback could be conducting chemical treatment on high-consistency (HC) refined TMP prior to low-consistency (LC) refining. Previously, we have shown that the treatment of TMP with oxidizing agents, such as highly alkaline hydrogen peroxide, oxygen and ozone, improves the tensile strength of TMP and protects the fibres from cutting during subsequent LC refining (Chang et al. 2010, 2011, 2016; Sun et al. 2016). The combination of oxidation and LC refining can result in a total energy savings to a given tensile of about 1000 kWh/t. We are investigating chlorine dioxide as a potential oxidizing agent for this treatment. As well as being an effective oxidizing agent, chlorine dioxide selectively reacts with lignin, and thus, should allow the treated pulp to maintain a high yield. Adequate tensile strength gains were found through chlorine dioxide treatment of TMP; however, significantly more tensile strength gains were found when chlorine dioxide-treated TMP was either soaked in sodium hydroxide caustic or bleached with alkali peroxide.

Effects of chlorine dioxide treatment, caustic soaking and peroxide bleaching on the properties of TMP

High freeness hemlock pulp, collected after secondary stage HC refining, was chelated to allow alkali peroxide treatments to be investigated in conjunction with chlorine dioxide. In the chlorine dioxide trials, we varied temperatures from 25°C to 65°C, time from 10 to 60 minutes, and chlorine dioxide charge from 1 to 5 percent, while the treatment consistency remained at 10 percent. After each trial, part of the treated pulp was soaked in caustic at 0.4 percent sodium hydroxide charge, temperature of 25°C, and a 4 percent pulp consistency for a total of 60 minutes each. Another portion of the treated pulp was bleached with alkali peroxide at 70°C with 4 percent peroxide charge and 4 percent sodium hydroxide charge for 90 minutes.

Figure 1 shows that chlorine dioxide treatment immediately affects the tensile of the pulp. After 10 minutes of treatment, the tensile index increased by 7 N·m/g. Further increase of treatment time had negligible effect on any strength gains of the pulp. Figure 1 also shows that when the treated pulp was soaked in sodium hydroxide, the tensile index increased by an additional 10 N·m/g to a total of about 17 N·m/g of improvement in comparison to the untreated control. When the untreated pulp was soaked under the same caustic conditions, but without prior chlorine dioxide treatment, tensile index only increased by 2 N·m/g. When the treated pulp was bleached with peroxide instead, the resulting tensile index values were very similar to those of treated and caustic soaked pulp. However, without chlorine dioxide treatment, peroxide bleaching of the control yielded a much higher tensile than that of the caustic-soaked control.

The brightness of the pulp decreased by 13 ISO after chlorine dioxide treatment (figure 2). The loss occurred after ten

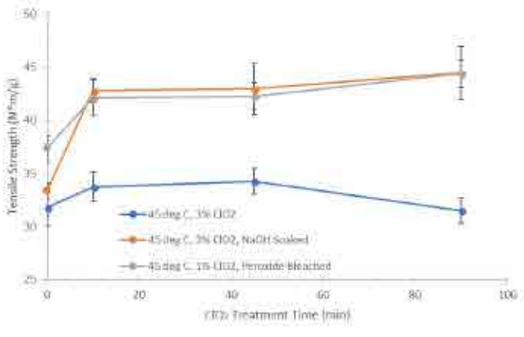

Figure 1: Effect of chlorine dioxide treatment time on tensile index of TMP, including effect with additional caustic soaking, and effect with additional peroxide bleaching.

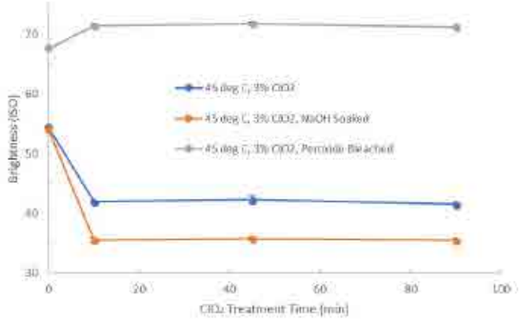

Figure 2: Effect of chlorine dioxide treatment time on brightness of TMP, including effect with additional caustic soaking, and effect with peroxide bleaching.

PROJECT 1.3

minutes and further treatment time had no further effect on the brightness of the pulp. When the treated pulp was soaked in caustic the brightness lowered by another seven ISO. The decrease in brightness compared to that of the untreated control was 20 ISO in total. When the untreated pulp was soaked in caustic without prior chlorine dioxide treatment the brightness was reduced by only two ISO. This drop in brightness with caustic soaking can be supported by prior work, where tests found that a higher pH was correlated with lower pulp brightness (Chang et al. 2016). On the other hand, the brightness of the pulp increased significantly for the peroxide bleached pulp. Furthermore, chlorine dioxide treatment prior to peroxide bleaching added to the increase in brightness, which demonstrates that a two-stage chlorine dioxide and peroxide treatment can improve pulp brightness up to 15 ISO.

Testing the hypothesis that acid generation causes tensile strength increase

We hypothesized that chlorine dioxide generated carboxylic acid groups when reacting with the pulp, causing swelling of the fibres and fines, and therefore increasing the tensile strength of the pulp. To test our hypothesis, we used conductometric titration. In this process, we converted acid groups within the pulp to acidic form by soaking the pulp in hydrochloric acid. We then slowly titrated 3 g OD (oven dry) of pulp dispersed in 450 mL of 0.001 M sodium chloride with sodium hydroxide (NaOH) while checking its conductivity every 5 minutes.

As sodium hydroxide is added, it consumes the protons in the suspension and decreases the conductivity (figure 3). When the sodium hydroxide has consumed all the free protons in solution, the conductivity remains constant as the carboxylic acids secreted within the fibre walls are neutralized. After the carboxylic acids are fully neutralized, the additional sodium hydroxide increases the conductivity of the solution. The volume of NaOH added while the conductivity remains constant corresponds to the carboxylic acid group content of the pulp.

Tensile strength is gained as the acid group content of the pulp increases. The chlorine dioxide treated pulps have higher acid group contents and tensile strengths than the untreated control pulps. A positive correlation between acidic group content and tensile index is consistent with our hypothesis that the generation of acid groups with chlorine dioxide treatment increases the tensile strength of TMP.

Testing the hypothesis that chlorine dioxide treatment exhibits low yield loss

One of the advantages of chlorine dioxide is that it selectively reacts with lignin instead of cellulose. We hypothesized that our chlorine dioxide treatment on TMP will cause little to no yield loss within the pulp. We investigated yield loss by measuring the chemical oxygen demand (COD) of the untreated and treated pulps. A COD value is a measure of how much water-dissolved oxygen can be consumed by decomposing organic matter in the presence of potassium dichromate. This means that the COD, or oxygen consumed, is directly related to how much organic matter has been dissolved. The amount of dissolved organic matter is related to yield loss during the treatment. In other words, there is a relationship between COD and pulp yield loss. The following relationship given by Genco et al. (2000) was used in determining our yield loss values.

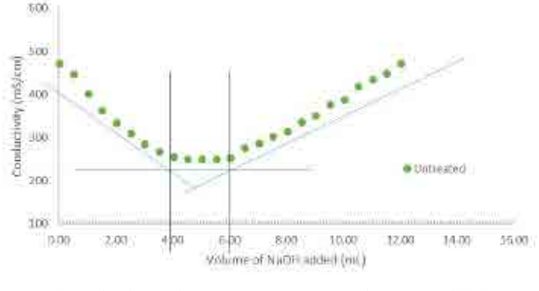

Figure 3: Example of a conductometric titration curve for untreated TMP, where the blue lines act as guides to outline the direction of the curve and the difference between the vertical lines represents the volume of NaOH required to neutralize acid groups within the pulp fibres.

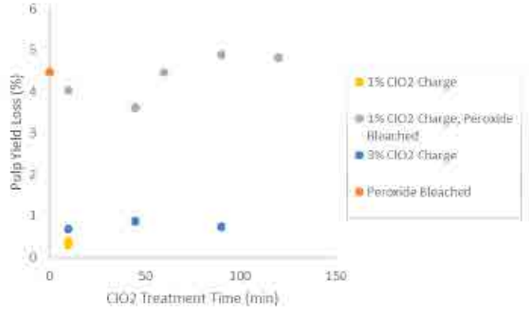

Figure 4: Effect of chlorine dioxide treatment, peroxide bleaching and combined treatment on pulp yield loss of TMP.

PROJECT 1.3

$$\delta\,(yield\ loss,\%) = 0.046 * COD\left(\frac{kg}{ton\ of\ pulp}\right)$$

Chlorine dioxide exhibited very low yield loss values of about 0.5–1.0 percent (figure 4). In comparison, when alkali peroxide treatment was also performed on the pulp, the yield loss was significantly higher, reaching to values of about 4–5 percent. Because chlorine dioxide treatment had an insignificant effect on the pulp yield, our hypothesis was proven correct.

References

Chang, X.F., C. Bridges, D Vu, D. Kuan, L. Kuang, J.A. Olson, and R.P. Beatson. 2010. "Saving electrical energy by alkaline peroxide treatment of TMP prior to low consistency refining". *Journal of Pulp and Paper Science*, 36(3–4): 129–134.

Chang, X. F., A. Luukkonen, J.A. Olson, and R.P. Beatson. 2016. "Pilot-scale investigation into the effects of alkaline peroxide pre-treatments on low-consistency refining of primary refined softwood TMP". *BioResources*, 11(1).

Chang, X. F., M. Miller, Y Sun, J.A. Olson, and R.P. Beatson. 2016. "A pilot scale comparison of the effects of chemical treatments of wood chips on the properties of high freeness TMP". Proceedings of the *International Mechanical Pulping Conference, September 26–28*, 362. Jacksonville, Florida, USA.

Chang, X.F., J.A. Olson, and R.P. Beatson. 2011. A comparison between the effects of ozone and alkaline peroxide treatments on TMP properties and subsequent low consistency refining. *BioResources,* 7(1): 99.

Genco, J.M., K.D. Zorn, and B. Cole. 2000. "Estimation of pulp yield loss in oxygen delignification using COD measurements". Paper presented at the *TAPPI Pulping Conference, November 5–8*. Boston, MA, USA.

Yu, S., M. Miller, X.F. Chang, J.A. Olson and R.P. Beatson. 2016. A pilot-scale comparison of the effects of chemical pre-treatments of wood chips on the properties of low consistency refined TMP. Proceedings of the *International Mechanical Pulping Conference, September 26–28,* 305–416. Jacksonville, Florida, USA.

JORGE RUBIANO

1.4 - OPTIMAL LOW CONSISTENCY REFINING

Our research developed key components to further understand the mechanisms of low consistency (LC) refining. First, we described fibre shortening, an important aspect in pulp production, using a statistical model. Second, we related the refining power consumption to machine and process variables. Third, we merged the two frameworks to analyze and assess refining systems commonly found in industry.

Comminution model

The size reduction of particles is a three-dimensional problem; however, its rigorous mathematical analysis is complex. The problem can be simplified to an idealized one-dimensional case under certain assumptions. In the case of size reduction of wood pulp fibres due to LC refining, the problem can be simplified to an idealized one-dimensional case since fibres have a high aspect ratio (between 30 and 100) and size reduction practically occurs along the fibres' length. Hence, size reduction of wood pulp fibres is often referred to as fibre shortening. Size reduction of cellulosic fibres can be studied by using a comminution model to describe the cutting mechanisms in terms of cutting rate S_i and cutting location B_{ij}. The comminution model equation written in terms of refiner radius is:

$$\frac{Q}{\omega}\frac{1}{4\pi\alpha\beta}\frac{1}{r}\frac{\mathrm{d}y_i}{\mathrm{d}r} = -S_i y_i + \sum_{j=1}^{p} B_{ij} S_j y_j$$

Where Q is the volumetric flow rate, ω is the refiner rotational speed, $\alpha = B/(B+G)$ and $\beta = 2GD/(B+G)$ with B, G and D representing bar width, groove width and groove depth respectively. Fibre length distribution (FLD) data from before and after refining with a variety of pulp types, net-powers, feed flow rates, rotational speeds and plate geometry was analyzed. We used this data to estimate selection function and breakage function.

Over the range of variables explored, we found certain correlations between parameters, specifically:

- The cutting rate was mainly dependent on the refiner gap. A power-law relationship well describes the dependency of cutting rate on the inverse of the gap.
- There is a clear indication that closing the gap favours fibre cutting in the middle points of fibres, whereas wider gaps promote a more evenly distributed cutting along the fibre length.
- We found evidence that plate geometry affects the cutting location. Coarser plates promote a more evenly distributed cutting whereas finer plates tend to cut more towards the middle of fibres.
- Long fibres are cut to a higher degree than short fibres.

Power–gap relationships

LC refining processes have been traditionally controlled and evaluated in terms of pulp and handsheet properties. The majority of refining studies take this approach to show how pulp properties are affected by refining. Alternatively, other studies have gone more into detail to understand the role of plate geometry, forces and energy in the overall refining operation. In contrast, to assess the same situation from a different perspective is atypical; for example, to understand the response of refiner behaviour to common variables such as pulp type and its changes, plate geometry, rotational speed and refiner diameter. This approach is important in cases where optimization of energy consumption for a particular refining operation is desired. Moreover, at an industrial scale, it is a daily occurrence where refiners operate at a wide range of conditions due to changes in feedstock properties and process conditions (e.g. flow rate or temperature changes). The description and understanding of the net-power-gap (referred to as power-gap) relationships are vital steps towards the optimization of any refining operation because they directly relate to the refining energy consumption.

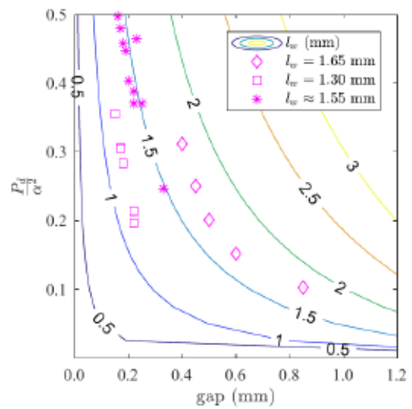

Figure 1: Contour plot of dimensionless power as a function of gap. Lines correspond to constant values of l_w as indicated. The plot was constructed using the fitted constants l_w°, c_1 and c_2. Data points correspond to industrial-scale-data used to validate the correlation.

PROJECT 1.4

We developed a dimensionless correlation from a basic analysis of bar-bar crossing power consumption relating important refining variables (refiner dimensions, plate geometry and rotational speed) with gap and fibre length as:

$$\frac{P_d}{\omega^2} = \left(\frac{l_w}{l_w{}^o}\right)^{c_1} G^{(2-c_2)}$$

Where P_d is dimensionless power, l_w is length-weighted mean fibre length, G = (gap0/gap -1) and $l_w{}^o$, c_1 and c_2 are fitting constants and gap0 is the gap at no-load-power. The fitting constants were estimated from a total of 151 data points from different pilot scale refining trials. In general, we found a good fit is R^2 = 0.936 and RMSE = 0.0514, considering the wide range of refining conditions, pulp types and plate geometries included in the data. Additionally, the error bars were rather short (between 2–8%), and confidence intervals of the fitted parameters were significantly narrow. The fitting results also suggest that the power-gap relationship is of the form $P_d \sim l_w^3$ and $P_d \sim G$. This developed correlation was tested to determine whether it could clearly describe data from both pilot plant-scale and industrial-scale refiners. Power-gap curves from a 72" double-disc refiner and a 58" double-disc refiner were measured using pulps with a l_w of 1.30 mm and 1.65 mm respectively. Additionally, power-gap values were collected from a 72" double-disc refiner using different operational conditions; for this collection of points the pulp had a l_w of 1.55 mm. Industrial scale data was plotted alongside the contour plot built from the developed correlation, and is shown in Figure 1. As can be seen, the correlation built upon pilot-scale data well describes the behaviour of industrial-scale data.

Refining systems analysis

A system composed of an LC refiner is a complex system to analyze since it is by nature a heterogeneous process involving heterogeneous raw material. Additionally, developing a

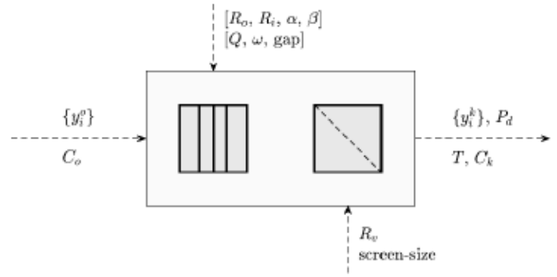

Figure 2: Block diagram showing an arbitrary model. Input variables: gap, volumetric reject ratio, R_v, initial pulp fibre length distribution, $\{y_i{}^o\}$, and consistency, C_o. Fixed parameters: screen size, refiner size, plate geometry, flow rate and refiner rotational speed. Output variables: fibre length distribution and consistencies, $\{yi^k\}$ and C_k, refining power, and thickening ratio, T.

mathematical model capable of accurately describing certain pulp properties changes due to refining is challenging. Part of the difficulties faced during modelling is that often times the properties of interest are not conservative (e.g. tensile, bulk and freeness). On the other hand, modelling conservative properties (e.g. fibre length) is an easier task. In the case of fibre length, models actually describe FLD changes using mass balances as a main tool of analysis.

Screening models, the developed comminution model and refining power correlation were implemented in the MATLAB Simulink toolbox. We used this environment to simulate three different refining systems. The systems consisted of one LC refiner and one pressure screen arranged in different configurations, namely "reject-refining", "feed-back rejects" and "feed-back reject-refining". Figure 3 gives details on the configurations and descriptions.

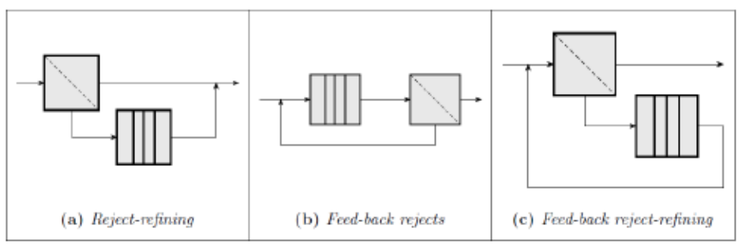

Figure 3: Block diagrams of the three refining systems studied.
(a) Reject-refining: Initial pulp is screened and the reject fraction is then refined and re-combined with the accept fraction.
(b) Feed-back rejects: Initial pulp is refined, then fractionated and the rejects are pumped back to the refiner inlet.
(c) Feed-back reject-refining: Initial pulp is screened and the reject fraction is then refined and pumped back to the screen feed.

RESEARCH UPDATES

PROJECT 1.4

For all systems, the input variables were fixed to gap=[0.2, 2.0] mm and Rv=[0.1, 0.5]. We set the initial flow and feed to the refiner at 4 percent consistency, because the comminution model was built on refining data at that consistency. The fibre length distributions were determined for each single flow of the system. We then calculated length-weighed mean fibre length values from the distributions to construct performance curves for each system.

In general it was found that recirculation considerably affects the system performance. It enables achieving higher energy contents but also decrease fibre length significantly. Combining refining and screening allows to increase the fibre length feeding the refiner and thereby increasing the loadability.

Specifically, for each system we found:

- Reject-refining could be beneficial in cases where the pulp can go through at least two refining stages in series. Moreover, pulp can undergo harsh treatments without excessive fibre shortening as only the coarse long fraction of pulp is refined. This system, in particular, has high throughputs compared to the refiner's capacity.
- Feed-back rejects could be suitable for applications requiring gentle treatments (wide gaps) or where only a single stage of refining is possible since it can achieve high energy contents. However, the system throughput is significantly lower compared to the refiner's capacity.
- Feed-back reject-refining could be regarded as a hybrid between the previously mentioned two systems. This hybrid achieves relatively high energy contents without excessive fibre shortening. This system could be suitable to reduce shives efficiently, and develop properties of the coarse material.

HUI TIAN

2.1: OPTIMIZATION AND CONTROL OF INTEGRATED HC AND LC REFINING

Background and objective

Mechanical pulping (MP) is one of the most energy-intensive processes in the pulp and paper industry, with the development of control strategies for MP processes dating back to the mid-1970s. Research has progressed significantly in areas such as refining optimization, energy reduction, and pulp quality improvement; driving the development of new control and optimization techniques to reduce energy consumption and enforce strict pulp quality specifications. Our objective is to reduce energy consumption and variability of pulp quality by developing novel advanced control and estimation techniques for a multi-stage high consistency (HC) and low consistency (LC) refining process.

Summary of previous work

We built a Winner-type nonlinear model for a two-stage (primary and secondary) HC refining process. Mechanical pulping is a complex multi-input, multi-output (MIMO) nonlinear process with strong interactions between the variables. In this two-stage MP model, the production rate, motor loads and consistencies for both primary and secondary refiners were chosen as the discretized differential state variables, whereas the pulp properties after each refiner stage were treated as algebraic state variables. The chip-transfer screw speed, plate gap and dilution water flow rates of each refiner were taken as the manipulated variables. The linear dynamics of the discretized differential state variables and their disturbances were modelled using data collected from several identification experiments on industrial processes.

The discrete-time nonlinear model for the two-stage MP process at time instant *t* can be written as,

$$\begin{aligned} x_{t+1} &= f(x_t, u_t) + w_t \\ y_t &= g(x_t) + v_t \end{aligned}$$

$$u_t = \begin{bmatrix} \text{Chip-transfer screw speed, } R \\ \text{Primary refiner plate gap, } G_p \\ \text{Primary dilution flow rate, } D_p \\ \text{Secondary refiner plate gap, } G_s \\ \text{Secondary dilution flow rate, } D_s \end{bmatrix}$$

$$x_t = \begin{bmatrix} \text{Production rate, } P \\ \text{Primary motor load, } M_p \\ \text{Primary consistency, } C_p \\ \text{Secondary motor load, } M_s \\ \text{Secondary consistency, } C_s \end{bmatrix}$$

where x, u_t, and y_t are the state variable, manipulated input variable, and output variable, respectively. The system nonlinear functions are denoted by $f(\cdot)$ and $g(\cdot)$, and w_t and v_t are the model uncertainty and measurement noise. The schematic of a two-stage HC refining process is shown in Figure 1.

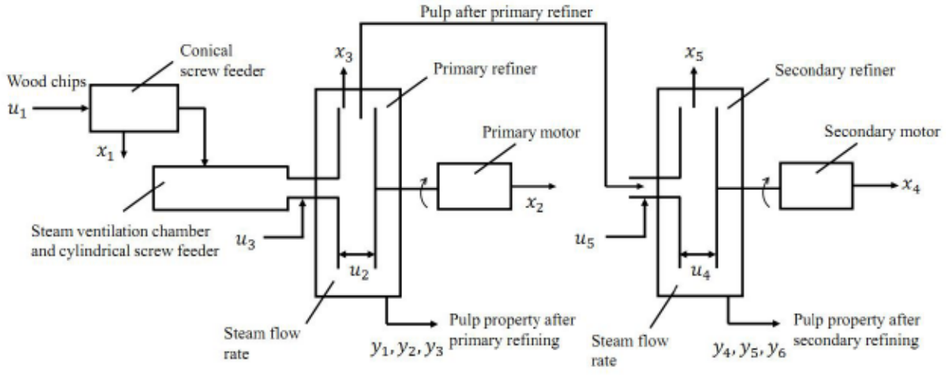

Figure 1: Schematic of a two-stage HC refining process.

PROJECT 2.1

Based on the developed nonlinear process model in equation 1, we completed the following model-based advanced control design. Computational time forms one of the most important concerns in implementing online control and estimation techniques in the actual MP production line. Reduction in computational time improves robustness of the nonlinear optimization problem. Our research used AMPL (A Mathematical Programming Language) and IPOPT (Interior-point OPTimizer) to investigate and solve this issue.

Economic model predictive control design

In the economic model predictive control (*econ* MPC) technique, the specific energy, defined as the ratio of production rate to the motor load, is considered the objective function. Two types of different regularization terms were added in the nonlinear *econ* MPC formulation to guarantee the convergence and stability of the nonlinear system. One penalizes the deviation of the states and inputs from their setpoints while the other penalizes the deviation of the states from their setpoints and the increment of two consecutive input variables. Moreover, to meet the process safety and pulp quality requirements, constraints for both manipulated variables and controlled variables were considered in the control of the MP process. We demonstrated that both the *econ* MPC schemes achieved significant reduction in specific energy consumed.

However, in order to reduce the specific energy used, a large weighting penalty had to be added to the economic term in the objective function. Another outcome was the significant deviation of the state variables from a steady-state target. Similar issues have also been reported in literature (H.Tian et al., 2016; Harinath et al., 2011 and 2013). These challenges motivated us to develop the *m-econ* MPC, which achieved an acceptable compromise between the tracking performance and the cost.

Multi-objective economic model predictive control

An auxiliary tracking MPC controller and a stabilizing constraint were incorporated in the *econ* MPC scheme to create the multi-objective economic model predictive control (*m-econ* MPC) technique. The stability of *m-econ* MPC is achieved by preserving the inherent stability of the auxiliary MPC controller. We defined a tuning parameter $\sigma \in [0,1)$ in the *m-econ* MPC dynamic optimization problem formulation which trades between tracking performance of the *m-econ* MPC controller and energy reduction rate. We demonstrated, from analysis and simulation results, that *m-econ* MPC has the following properties:

- For fixed state variable, *m-econ* MPC is feasible for all $\sigma \in [0,1)$.
- When $\sigma = 0$, *m-econ* MPC will be reduced to be a standard tracking MPC. When $\sigma = 1$, *m-econ* MPC is an *econ* MPC without any regulation terms, that is, the stability or the convergence cannot be guaranteed.
- The tracking MPC and *econ* MPC can be interpreted as two special cases of *m-econ* MPC techniques.
- *M-econ* MPC can achieve 12–24 percent reduction in specific energy.

Moving horizon estimation design

Our previous research on econ MPC and m-econ MPC assumed that state variables and the pulp properties were available at all times. However, the state is rarely available directly from process measurements and typically needs to be inferred from secondary process measurements or a measurable subset of the state. Even when the state is directly accessible, one still needs to address measurement noise. If the model uncertainty is significant or if accurate estimates are required, then the state estimator must account for uncertain parameters or process variations.

Building on our previous research on the *m-econ* MPC algorithm for a two-stage HC MP process, we employed the well-known moving horizon estimation (MHE) technique to the nonlinear MP process. MHE is a practical and efficient optimization-based strategy for state estimation that explicitly allows for nonlinear models and inequality constraints. The basic philosophy of MHE can be summarized as follows:

- Estimates of the states are obtained by solving a least squares problem, which penalizes the deviation between measurements and predicted outputs of a system.
- When the state is estimated at the next time index, the

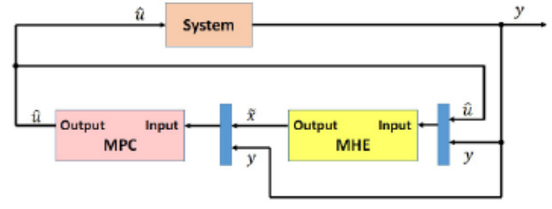

Figure 2: Graphical depiction of the integrated MPC and MHE for MP process.

PROJECT 2.1

new measurement is added to the data window and the oldest measurement is removed.

Simulations show that MHE can provide a good estimation of measurable but noisy states (production rate and motor loads) and unmeasurable states (consistency) for both primary and secondary HC refiners. The final integration of our proposed MPC and MHE technique can be found in Figure 2.

Stochastic economic model predictive control

We developed a robust scenario-based stochastic economic model predictive control (SSEMPC) to reduce the variability of the state variables and the pulp properties for a MP process. Traditional MPC in literature, both for linear and nonlinear processes, is usually based on the assumption that the process model is accurate and that future disturbances are constant [1-3]. However, these assumptions are not valid in practice and can result in poor closed-loop performance if the disturbances vary over time, if a model–plant mismatch is present, or some combination of both. In the scenario-based stochastic m-econ MPC techniques, the system dynamics are of a stochastic nature, and an additive disturbance is introduced to represent the uncertainties in the system model. This additive disturbance is a continuous random variable and its true probability distribution is often approximated by discrete probability scenarios. Stochastic optimizations, which are complex to solve, are usually employed for the control design with the stochastic models. However, with scenario-based optimization techniques, we can avoid the challenges associated with stochastic optimizations by decomposing the problem into a set of similar deterministic optimizations that can be efficiently solved using parallel computation.

Future research plans

We visited Alberta News Print Company, Whitecourt, Alberta on 23 and 24 October 2017, and collected the MPC controller data. Our next research goal is to validate our proposed control techniques in a pulp mill. Moreover, MHE will make it possible for us to apply the control technique in a pilot trial or in pulp mills where only limited sensors are available. Our workflow continues as outlined:

- Understand the process and MPC controller in the pulp mill.
- Simulations: apply *m-econ* MPC to the existing process model and compare the simulation results.
- Run *m-econ* MPC in parallel to the MPC in the pulp mill
- Replace the traditional MPC with our *m-econ* MPC.
- Put *m-econ* MPC in production.

We will finalize our collaboration plans with the partner mills.

References

Tian H., Q. Lu, R.B. Gopaluni, V.M. Zavala, and J.A. Olson. 2016. "Economic nonlinear model predictive control for mechanical pulping process." Accepted at the *American Control Conference, July 6–8*, Boston, MA, USA.

Harinath E., L.T. Biegler, and G.A. Dumont. 2011. "Advanced step nonlinear model predictive control for two-stage thermo mechanical pulping processes." *World Congress*. 18(1):3653–58.

Harniath E., L.T. Biegler, and G.A. Dumont. 2013. "Predictive optimal control for thermo-mechanical pulping process with multi-stage low consistency refining." *Journal of Process Control*. 23(7):1001–11.

REZA HARIRFOROUSH

2.2: LOW CONSISTENCY REFINER BAR FORCE SENSOR BASED CONTROL STRATEGIES

We used custom-built piezoelectric force sensors to detect the onset of fibre cutting, in real time, in low consistency (LC) refining. Detection of the onset of fibre cutting is potentially beneficial as part of a control system to reduce fibre cutting and increase energy efficiency. The sensors were installed in an Aikawa pilot-scale 16-inch, single-disc refiner at the Pulp and Paper Centre at the University of British Columbia. Trials were performed using different pulp furnishes (i.e. softwood and hardwood), refiner plate patterns at different rotational speeds, and a wide range of plate gaps. Pulp samples were collected at regular intervals, and pulp and paper properties were measured. Based on time and frequency domain analysis of sensor data, we identified fibre cutting metrics that detected the onset of fibre cutting in real time (Harirforoush et al. 2017, 2018). Moreover, we investigated the effect of pulp furnish and plate pattern on bar forces (Harirforoush, Olson, Wild 2018).

Recirculation is commonly used in LC refining to maintain fibre flow through the refiner. The effect of flow recirculation on pulp properties and energy efficiency was studied in 2015 (Sandberg, Berg 2015). However, the effect of continuous recirculation mode on mechanical interactions between refiner bars and pulp fibres, which ultimately influences pulp properties, has not been investigated. This study investigated the effect of recirculation on the relation between bar forces, refiner control variables, and pulp properties using the refiner force sensor that measures forces applied to a short segment of a bar on the stator.

Trials were conducted with the plate having a BEL of 5.59 km/rev operating at 1200 rpm. Spruce-pine-fir softwood thermomechanical pulp (SPF SW TMP) and northern bleached softwood kraft pulp (NBSK) were used in these trials. During the trials, either power or plate gap was held constant; the pulp was recirculated through the refiner numerous times, with samples taken randomly to measure pulp properties (i.e. length-weighted fibre length).

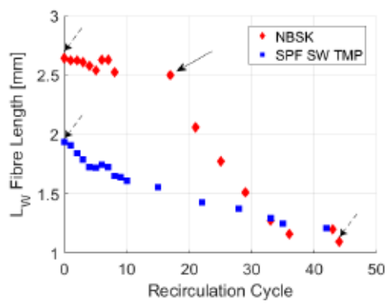

Figure 1: Length-weighted fibre length versus the number of recirculation cycle. The no-load data is highlighted by dashed arrows. The critical gap is highlighted by a solid arrow.

Operating at constant gap (0.35 mm)

As is shown in Figure 1, with NBSK pulp, the length-weighted fibre length (L_w), remained relatively constant until the 17th recirculation cycle was completed. Beyond this point, the fibre was cut and L_w decreased. SPF SW TMP pulp, however, showed no such distinct transition. Rather, L_w decreased continuously. It was observed that the critical gaps were 0.30 mm and 0.39mm for NBSK and SPF SW pulps respectively, as determined from fibre length data and the algorithm explained in (Harirforoush, Olson, Wild 2018).

As shown in Figure 2a-b, for NBSK pulp, mean peak normal and shear forces were relatively constant up to the recirculation cycle at which the critical gap occurred, as indicated by the solid arrow in Figure 1. Beyond this critical gap, the mean peak forces decreased. However, for SPF SW TMP, mean peak normal and shear forces remained relatively constant throughout the entire trial.

Operating at constant power

L_w versus recirculation cycle is shown in Figure 3. NSBK pulp experienced fibre cutting after the 12th recirculation cycle was completed. SPF SW TMP saw a decrease in L_w continuously. The plate gap was approximately 0.35 mm for operations at constant power; however, after the first couple of recirculation cycles were completed, the plate gap continually decreased through the remainder of the trial.

The critical gap for NBSK pulp, indicated as the solid arrow in Figure 3, is determined by an increase in mean peak normal and shear forces. However, these forces increase slowly for SPF SW TMP pulp (Figure 4c-d).

Conclusion

In recirculation trials, when operating at gaps greater than the critical gap, fibre cutting occurs after a number of recirculation cycles are completed. Fibre cutting, at constant gap operation, was indicated by a decreasing trend in mean peak forces.

PROJECT 2.2

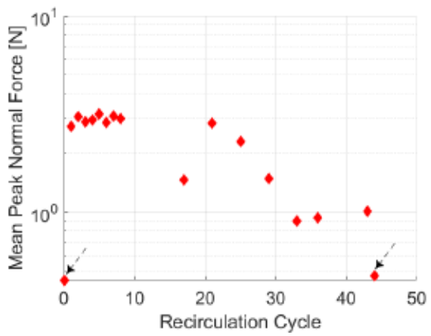

2(a)

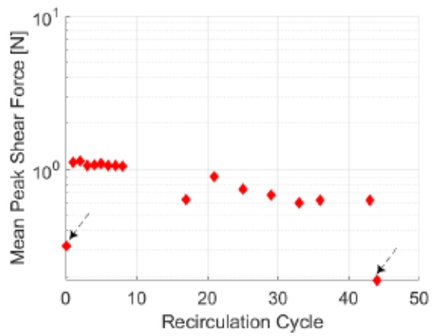

2(b)

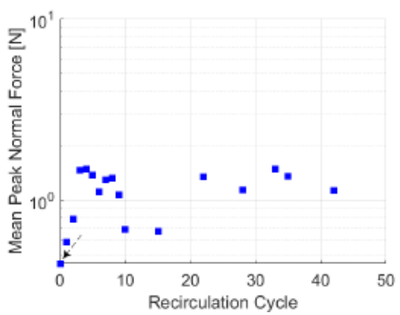

2(c)

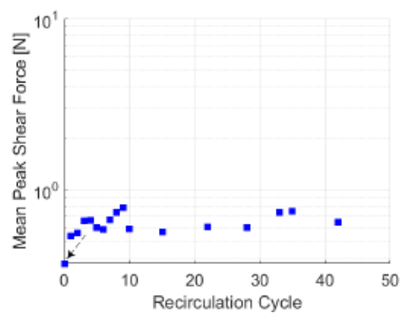

2(d)

Figure 2 (a, b, c,and d): Mean peak normal and shear forces versus the number of recirculation cycles for NBSK pulp (a, b), and SPF SW TMP pulp (c, d). The no-load data points are highlighted by dashed arrows.

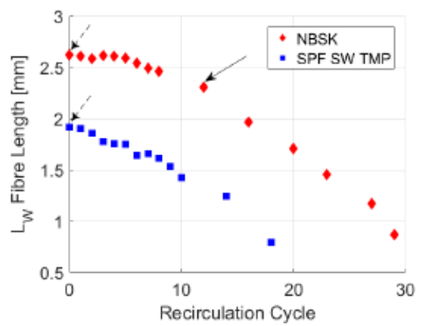

Figure 3: Length-weighted fibre length versus the number of recirculation cycle. The no-load data is highlighted by dashed arrows. The critical gap is highlighted by a solid arrow.

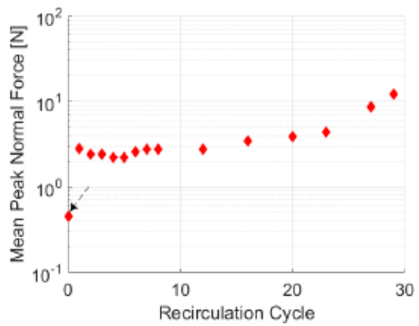

4(a)

Figure 4 (a,b,c and d): Mean peak normal and shear forces versus the number of recirculation cycles for NBSK pulp (a, b), and SPF SW TMP pulp (c, d). The no-load data is highlighted by dashed arrows.

PROJECT 2.2

However, when operating at constant power, fibre cutting was indicated by an increasing trend in mean peak forces. For operations at gaps below the critical gap, measured forces trended constant at constant gap. Though, for operations at gaps below the critical gap, measured forces trended upward at constant power. These results show that the sensor is able to detect the onset of fibre cutting in continuous recirculation mode in low consistency refining.

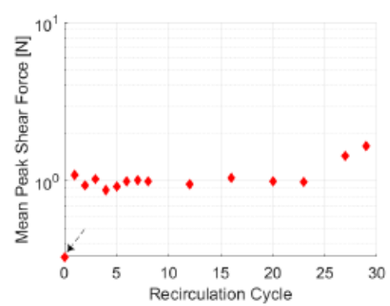

4(b)

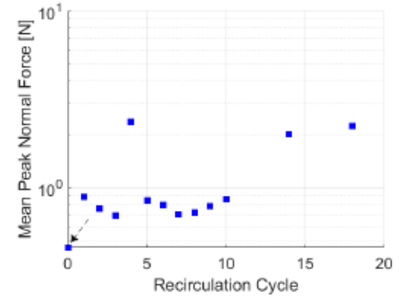

4(c)

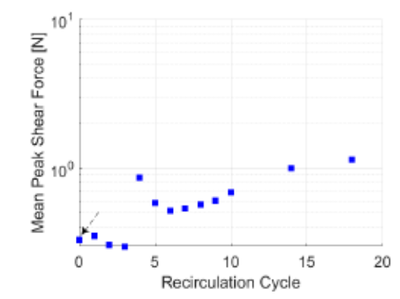

4(d)

Figure 4 (a,b,c and d): Mean peak normal and shear forces versus the number of recirculation cycles for NBSK pulp (a, b), and SPF SW TMP pulp (c, d). The no-load data is highlighted by dashed arrows.

References

Harirforoush, R., J.A Olson, P. Wild. 2017. "In-process detection of fiber cutting in low consistency refining based on measurement of forces on refiner bars." *TAPPI Journal*. 16(4): 189–99.

Harirforoush, R., J.A. Olson, P. Wild. 2018. "Indications of the onset of fiber cutting in low consistency refining using a refiner force sensor: the effect of pulp furnish." *Nordic Pulp and Paper Research Journal*. 33(1): 48–57.

Harirforoush, R., J.A. Olson, P. Wild. 2018. "Bar force measurements in low consistency refining: the effect of plate pattern." Accepted for publication in *Nordic Pulp and Paper Research Journal*.

Sandberg, C., and J-E Berg. 2015. "Effect of flow recirculation on pulp quality and energy efficiency in low consistency refining of mechanical pulp." *Nordic Pulp and Paper Research Journal*. 30 (2): 230–233.

MATTHIAS AIGNER

2.2: LOW CONSISTENCY REFINER BAR FORCE SENSOR BASED CONTROL STRATEGIES

Refiner control strategies were primarily based on global process variables such as rotational speed, flow rate, inlet pulp consistency and outlet fiber length (Luukkonen, 2010). In our previous research conducted by Reza Harirforoush, a force sensor was developed to directly measure forces applied by the pulp to the refiner bars to monitor and validate the mechanical interactions in the refiner chamber. This type of sensor is used in a variety of high consistency (HC) (Olender 2007) and low consistency (LC) (Prairie, 2008, Harirforoush 2016) refiners. Most recently, this sensor was embedded into plates of the AIKAWA 16" single disk pilot LC refiner at the Pulp and Paper Centre at the University of British Columbia.

We used this sensor to measure normal and shear forces applied to the refiner bars by the pulp under various process configurations. The addition of a rotary encoder to the UBC LC refiner is underway, and will provide further data on the angular position of the rotor during the refining process. The data will be used to determine the position of the bars of the rotor plate, relative to the bars on the stator plate.

The angular position of the refiner plates will be measured through a high resolution rotary encoder with a maximum of 65,536 pulses per revolution. The encoder is mounted as shown in figure 3, and will record the rotation of the drive shaft through a rubber coated wheel. A photoelectric sensor directed at the drive shaft will provide a synchronous pulse with each revolution to detect any slip of the rubber wheel.

The position of the rotor bars, relative to the stator bars, will be used in conjunction with the bar force data. Bar force data typically consists of a sequence of peaks as displayed in Figure 1, each of which corresponds to the passage of a bar on the rotor plate over the force sensor located in the stator plate. The data from the rotary encoder will be used to record these force peaks in combination with the position of the rotor bars as they pass over the sensor as shown in Figure 2. The data will be used to study the mechanics of the refining process at the point of interaction between the bars and the pulp. The knowledge over the geographic occurrence of the force on each refiner bar enables a better understanding of the components that lead to the shear forces measured by the force sensor.

A dry run of the rotary encoder (figure 3) was conducted on April 6 at the Pulp and Paper Center, and pilot scale trials are planned for the summer of 2018.

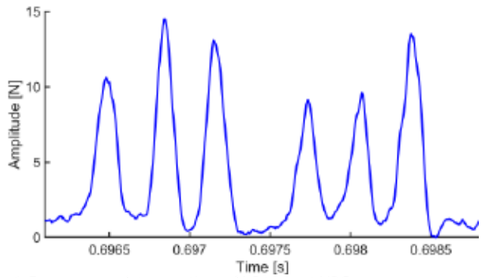

Figure 1: Force sensor data over time of LC tests at UBC.

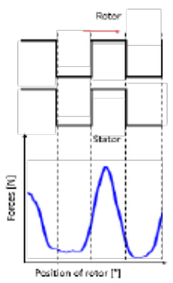

Figure 2: : Force sensor data in combination with anticipated position data of Encoder.

Figure 3: Encoder setup at the UBC test refiner.

References

Luukkonen, A., J.A. Olson, and D.M. Martinez. 2010. "Low consistency refining of mechanical pulp, effect of gap, speed and power." *Journal of Pulp and Paper Science*. 36, (1-2):28-34.

Olender, Dustin James. 2007. "Forces on bars in high-consistency mill-scale refiners." Dissertation. University of Victoria. https://dspace.library.uvic.ca/bitstream/handle/1828/297/Olender_Thesis_122407.pdf?sequence=1

Prairie, B., P. Wild, P. Byrnes, D. Olender, W. Francis, and D. Ouellet. 2008. "Forces during bar-passing events in low-consistency refining: distributions and relationships to specific edge load." *Journal of Pulp and Paper Science*. 34, (1):1.

Harirforoush, Reza, Peter Wild, and James Olson. 2016. "The relation between net power, gap, and forces on bars in low consistency refining." *Nordic Pulp and Paper Research Journal*. 31, (1):71-78.

BRYAN BOHN

2.3: ADVANCED PUMP PERFORMANCE MONITORING SYSTEM

Project overview

The objective is to develop improved sensing methods for measurement, analysis, control, and wear observation of centrifugal pumps. The intent is to minimize, through better measurement and performance prediction, energy consumption that results from inefficiency in pumping processes. Previously, project researcher Ramin Khoie developed an online magnetic sensor to observe material loss over time from the surface of a centrifugal pump impeller blade (Khoie et al., 2015). The externally-mounted device, shown in Figure 1, passes a magnetic flux through the pump housing and operating area of the impeller. Over time, as the impeller wears from use, the reluctance of the circuit increases. This creates a drop in the inductance of the circuit, which is measured and correlated to a known gap tolerance for the testbed pump.

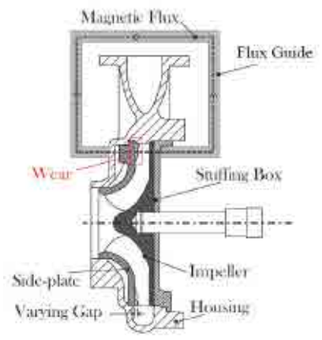

Figure 1: A magnetic sensor for measuring impeller wear.

Establishing pump efficiency

A literature review has been conducted to evaluate existing approaches and sensing technologies for actively measuring the efficiency of centrifugal pumps. Conventional testing typically measures power input to the driving motor, pressure at the pump intake and outlet, and fluid flow rate (Cattaert, 2007). These values are applied to equation 1, which states that the overall thermodynamic efficiency of a pumping system is the ratio of fluid work generated (W_{fluid}) to power consumed by the driving electric motor (W_{motor}) (ISO 5198, 1999).

$$\eta_{overall} = \frac{W_{fluid}}{W_{motor}} = \frac{\rho g q_V H}{W_{motor}} \qquad \text{Equation 1}$$

In this case, the work imparted to the working fluid is equal to the product of the fluid density (ρ), gravitational acceleration (g), volumetric flow rate (q_V), and pressure head change between the pump's intake and outlet (H).

An alternative and perhaps more practicable efficiency monitoring methodology is the thermodynamic method, which was implemented in a 2013 survey of municipal pumping infrastructure throughout Ontario (Papa et al., 2013). Unlike conventional pump efficiency testing, thermodynamic method measures fluid temperature at the pump intake and outlet, rather than fluid flow rate. In its simplest approximation, the method assumes that the electrical power input to the motor yields only fluid work and waste heat into the working fluid. By directly measuring the pumping energy lost as heat generation, an accurate determination of the pump's thermodynamic efficiency (η_{thermo}) can be made using equation 2 (Cattaert, 2007):

$$\eta_{thermo} = \frac{1}{1+\rho C_p(\Delta T - \Delta T_i)/(\Delta P)} \qquad \text{Equation 2}$$

Where ρ is the fluid density, C_p is the specific heat of the working fluid ΔT and ΔT_i are the temperature changes across the actual pump and an idealized isentropic pump respectively, and ΔP is the pressure change between the suction and discharge ports. The fluid work at the pump discharge is then calculated by multiplying the measured input power by the thermal efficiency. In suitable conditions, the thermodynamic method has been demonstrated to achieve efficiency measurements within two percent uncertainty (ISO 5198, 1999).

Meaningful measurement in the absence of well-defined pump parameters

It is noted that the thermodynamic method for centrifugal pump instrumentation is independent of pump geometry and can be applied to systems with unknown physical parameters and performance. This has the potential to be particularly valuable for industrial applications where the mechanical parameters of the pumping systems are not well-defined, either from previous modification, age, wear, or alterations of the surrounding flow system. It is proposed that using the thermodynamic method for instrumentation will provide a suitable base on which to develop an active pump performance monitoring system. Such an approach produces a direct,

PROJECT 2.3

accurate measurement of thermal efficiency, which can be correlated over an extended period of time into efficiency trends. These trends can be used to inform refurbishment schedules, target underperforming pumps for repair, track performance, and when feasible, optimize electrical power input to the driving motor.

Current research

A MATLAB centrifugal pump efficiency model is under development. The design of the simulation is shown as a simplified block diagram in Figure 2.

This numerical model differs from typical idealized motor-pump response models in that it is oriented toward measuring and understanding the impacts pumping system disturbances have on efficiency, as well as evaluating potential measurement methods. As with a physical pump, the simulated efficiency is a function of power input to the driving motor, bearing friction, pressure parameters at the pump suction and discharge ports, impeller diameter, wear condition, and other physical parameters. To measure the efficiency response, the MATLAB model implements a sensor system based on the thermodynamic method discussed above. This pump simulation will be valuable in the development of a small-scale pump efficiency monitoring testbed.

Partner collaboration

The UBC Advanced Pump Performance Monitoring System group had the opportunity to engage in three site visits with industry partners last fall and winter. In November 2017, Westcan Industries generously toured us through their facilities, and shared outstanding technical expertise on centrifugal pumps and pump monitoring systems. In January 2018, Catalyst Paper welcomed us to both their Port Alberni and Crofton facilities for tours. The visits provided an invaluable glimpse of the direct applications for the envisioned monitoring system.

References

Khoie, Ramin, Bhushan Gopaluni, James A. Olson and Boris Stoeber. 2015."A magnetic sensor to measure wear in centrifugal pumps." *2015 IEEE Sensors*: 1–4. Busan, South Korea.

Cattaert, A. E. 2007. "High Pressure Pump Efficiency Determination from Temperature and Pressure Measurements." *IEEE Power Engineering Society Conference and Exposition in Africa*. Johannesburg, South Africa.

BS EN ISO 5198:1999. 1999. "Centrifugal, mixed flow, and axial pumps – Code for hydraulic performance tests – Precision class." Standard, *International Organization for Standardization* (ISO), Brussels, Belgium.

Papa, Fabian, and Djordje T. Radulj. 2013. "Thermodynamic method used for pump performance and efficiency testing program." *Environmental Science and Engineering Magazine:* 44–48.

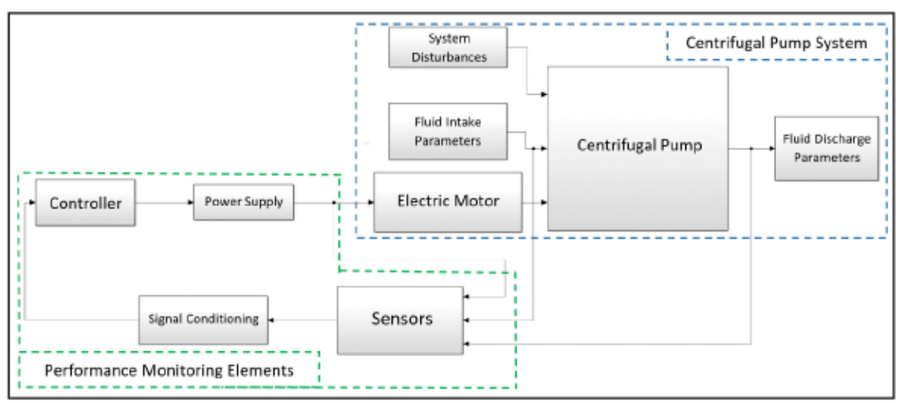

Figure 2: Elements of the centrifugal pump performance monitoring system simulation.

TARANEH KORDI

3.2: LOW CONSISTENCY REFINED PULP FOR PACKAGING INDUSTRIES

3.2 (A) Application of LCR in producing multi-ply folding boxboards

Our research focused on the performance of folding boxboards (FBB) as refining energy is reduced using screening and LC refining (LCR). Screening reduces refining energy by fractionating primary high consistency refined (HCR) pulp. Only the long fibre fractions (reject pulp) then undergo LC refining. Experiments on modelling studied the effects of fibres and fibre network variables on ply-bond strength.

Experiments

We examined the effects of lower energy consumption achieved by using LCR reject pulp and various screen designs on the physical and mechanical properties of resulting folding boxboards. Several 3-ply folding boxboards were prepared with different middle plies using hand-sheet maker. Basis weight of all samples were 210 g/m2 with 50, 40, 120 g/m2 for top, bottom, and middle layer, respectively. Quesnel River Pulp provided the HC refined SPF (spruce, pine, fir) pulp at 600mL freeness. The HC refined pulp had been either HC refined secondarily or fractionated, followed by LC refining at the ANDRITZ pilot plant in Springfield, Ohio. The fractionation was conducted using three different baskets with 0.8, 1, and 1.5 mm hole diameter. Unscreened pulp from the HC refiner and the screened reject pulps were LC refined at two intensities of 0.25 and 0.5 J/m. As control samples, we examined unscreened pulp refined with HCR-HCR and HCR-LCR at high and low intensity. The overall refining and screening outline is illustrated in Figure 1. The LC refined reject pulp at different freeness, as well as the accept pulp and unscreened pulps were shipped to the pulp and paper lab at the University of Toronto to produce the middle ply of the 3-ply FBBs.

Middle-ply was the combination of reject and accept pulp with a specific ratio according to the reject ratio obtained after screening. The freeness of middle-ply furnish of reject and accept pulp was measured at the University of Toronto. Pulp properties of middle-ply furnish—including fibre length, coarseness, fibre width and fine percentage—were measured using FQA test at UBC's Pulp and Paper Centre. Physical and mechanical properties of 3-ply FBBs including bulk, tensile, ply-bond strength, and tear strength were tested at University of Toronto (figure 2).

Bulk decreased as the middle ply freeness decreased. The highest bulk was observed for HCR-HCR, owing to preservation of long fibres (Figure 1a). Tensile index improved with LC refining as the freeness and length-weighted (LW) average fibre length decreased as a result of improving the fibre-fibre bonding, and produced a higher fines content through refining. At the same freeness, screening increased tensile index compared with the unscreened HCR-LCR refined samples. These results may be attributed to more uniform and higher long-fibre content of screened pulps and lower coarseness of LC refined samples compared to HCR-HCR (Figures 1b). Tear index increased, peaked, and dropped as freeness decreased. Tear index of all samples were in the range of 12 ± 3 mN.m2/g (Figure 1c). Ply-bond strength increased as freeness decreased by more refining and as smaller screen cylinders were applied, because of shorter fibres and more bonds (Figure 1d).

Modelling

We computationally examined the effects of fibres and fibre network properties on fibre bonding and ply-bond strength. By moving from the traditional cause-to-effect approach

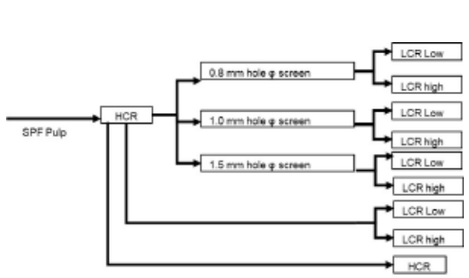

Figure 1(a): Outline of pulp refining.

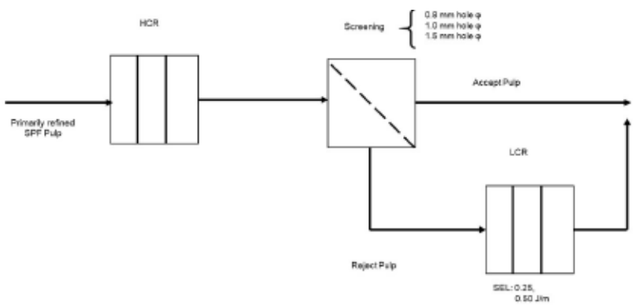

Figure 1(b): Outline of pulp screening.

PROJECT 3.2 (A)

(experimental work) to goal-to-means approach (modelling work), the numerous trials in laboratory, pilot plant, and paper mills could be reduced or eliminated, resulting in fewer experimental errors, and increased cost savings. In goal-to-means approach achieved by modelling, the final product or material was designed first with desired performance goals, and then the structure and process conditions was optimized to achieve the target performance. Moreover, modelling ply-bond test provided us with valuable information about the micro-mechanics of fibres and fibre bonds, and led to a better understanding of fibres behaviour during the testing analysis.

The fibres and fibre networks in the models were generated computationally and subjected to simulated ply-bond tests. We used a particle-based method, particularly, discrete element method (DEM) in ESyS-Particle software to model the fibre networks. Paraview software helped us visualize the micromechanics of the fibres and fibre networks. The simulations provided us with force data, which could then be compared with physical experimentation results, and the energy values of both the fibres and fibre-fibre bonds. Our models enabled us to study the micro-mechanics in fibre networks during the ply-bond test, and allowed us to predict ply-bond strength from fibre properties and network properties. These properties include average fibre length, fibre coarseness, fibre Young's modulus, fibre shear modulus, bond strength, basis weight, network porosity and network size.

Several 3-ply boards with total grammage of 60 g/m2 were generated. Each ply was 20 g/m2 and compressed to form a 3-ply fibre network. We investigated the effects of fibre-fibre bond strength and network density on the ply-bond strength. Various network densities were achieved by compressing the fibre networks to different levels. Various bond strengths were

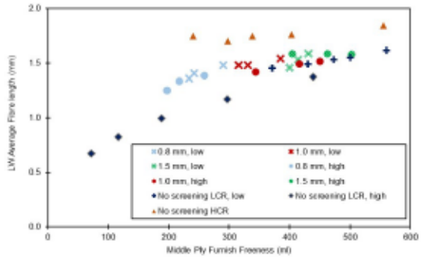

Figure 2: The effect of refining and screening on LW average fibre length of middle-ply furnish

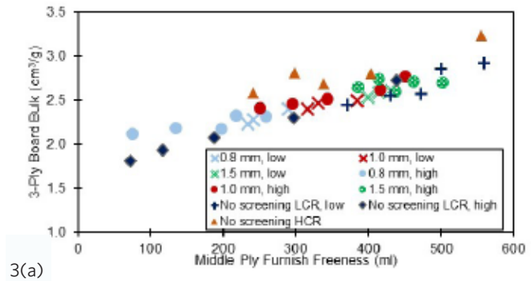

3(a)

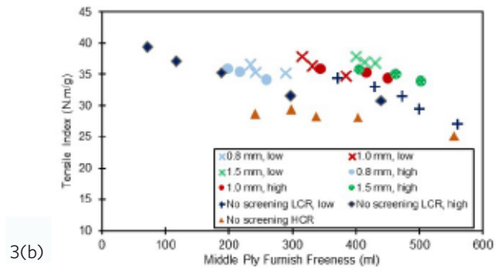

3(b)

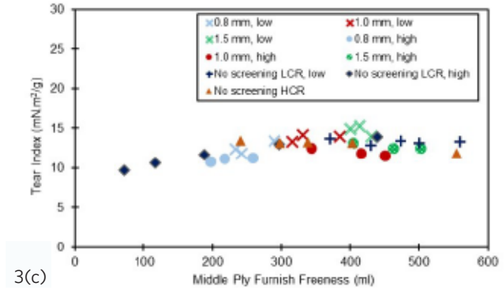

3(c)

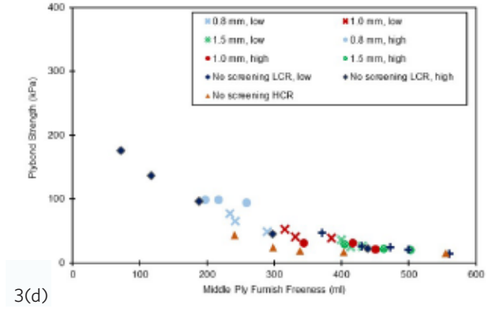

3(d)

Figure 3 (a, b, c and d): The effect of screen hole size, refining intensity, and pulp freeness used in the middle ply on (a) bulk (cm3/g), (b) tensile index (N.m/g), (c) tear index (mN.m2/g), and (d) ply-bond strength (kPa)

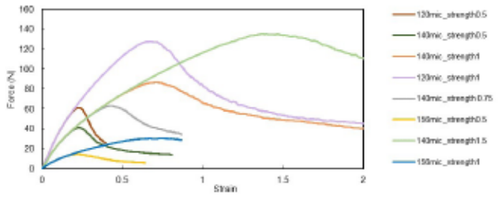

Figure 4: Force-strain results of the simulated ply-bond test for various board densities and fibre-fibre bond strength.

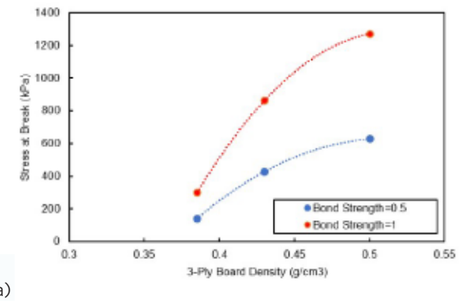

5(a)

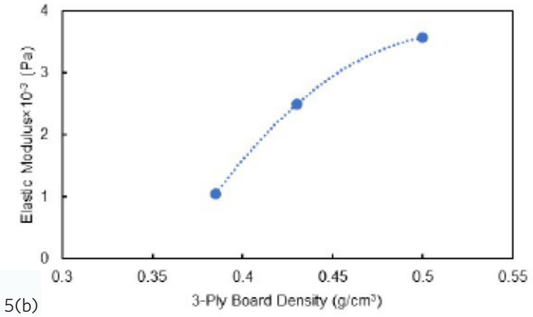

5(b)

Figure 5 (and b): The effect of board density on (a) ply-bond stress at break for various bond strengths; (b) elastic modulus.

achieved by multiplying force values required for fibre breakage by 0.5, 0.75, 1, and 1.5. The ply-bond test results of different network densities and bond strengths are shown in Figure 2. Figure 3 shows the effect of network density on the ply-bond test stress and elastic modulus. To speed up the computational process, we used the supercomputing facility available at the University of Toronto, SciNet, and Compute Canada.

Ply-bond stress at break increased as density increased, and its rate was higher for the higher bond strength. Higher bond strength resulted in higher ply-bond stress (Figure 3a). The elastic modulus of boards increased as the density increased, although its rate was lower at higher densities.

Next steps

Our future research aims to further investigate and study additional network densities and bond strengths to model the ply-bond strength as a function of density and bond strength. As well, 3-ply boards with different properties and higher grammages will be studied with our modelling system. This will allow us to study the effects of board grammage and model ply-bond strength based on fibre properties.

Acknowledgements

We are grateful to a number of researchers and technicians who helped us progress in our research as well as to companies.

- S. Hossain, P. Bergström and Prof. T. Uesaka of Mid Sweden University, Sundsvall, Sweden.
- Reanna Seifert and UBC work-learn student Jocelyn Zhou at UBC's Pulp and Paper Centre.
- And to SciNet and Compute Canada.

BAHAR SOLTANMOHAMMADI

3.2 (B): LOW CONSISTENCY REFINED MECHANICAL PULP FOR PRODUCING FLEXIBLE PACKAGING PAPERS

Flexible packaging papers (FPP), such as sack papers, available in the market are typically made of HCR-LCR sack kraft pulps due to their promising mechanical properties. These chemical fibres provide higher wet strength and consume less energy to manufacture compared with mechanical pulps. However, mechanical pulps including BCTMP (bleached chemi-thermal mechanical pulp), still have various benefits over chemical fibres, owing to their relatively low production cost and assuring yield. In order to obtain the advantages of both pulping processes in production of sack papers, BCTMP and sack Kraft pulp were LC-refined together at a specific ratio. The product of this combination can help maintain mechanical performance of current sack papers while reducing production cost and improving the yield.

Research and trials

Various blends of Canfor's HCR-sack kraft pulp and BCTMP, each made of 0%,10%, and 20% BCTMP, were co-LC refined under different refining conditions at Canfor Pulp Innovation (CPI) in Burnaby, British Columbia. Table 1 shows a summary of the LCR trials conducted.

Pulp Sample	0% BCTMP	10% BCTMP		20% BCTMP
SEL (J/m)	1.0	1.0	0.5	1.0
SRE (kWh/t)	0 40 80 120	0 40 80 120	0 40 80 120	0 40 80 120

Table 1: Sack Kraft and BCTMP co-LC refined trial targets for Specific Edge Load (SEL) and Specific Refining Energy (SRE).

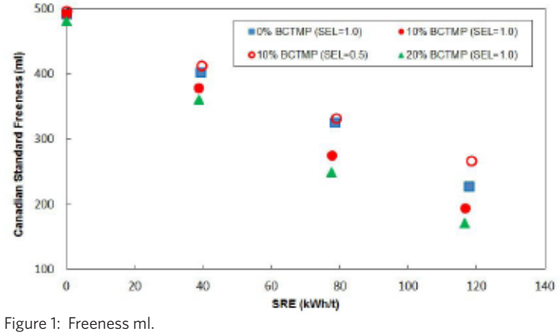

Figure 1: Freeness ml.

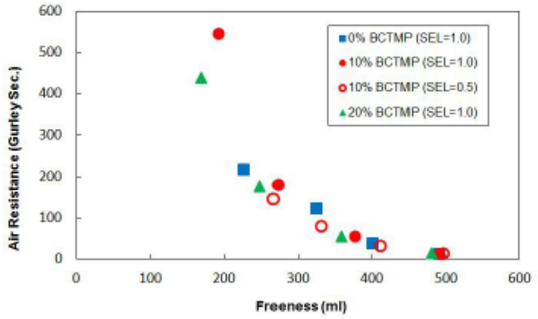

Figure 2: Air resistance.

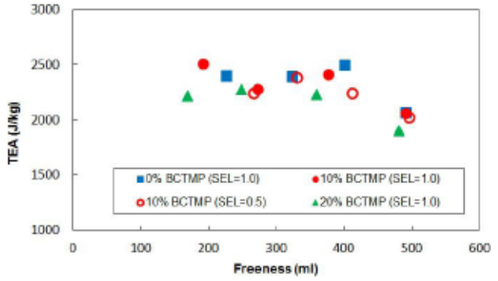

Figure 3: Tensile energy absortion j/kg.

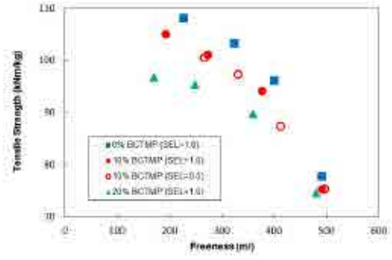

Figure 4: Tensile strength kNm/kg.

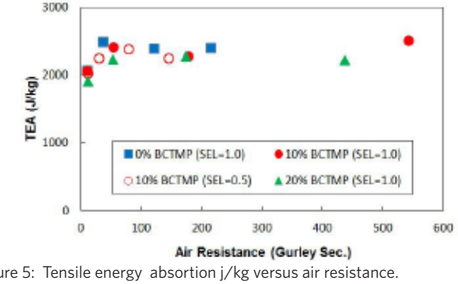

Figure 5: Tensile energy absortion j/kg versus air resistance.

Freeness of each refined pulp sample was tested. According to the freeness, handsheets containing only one layer of 60 g/m2 pulp were produced using the semi-automatic sheet former at CPI's wet lab. As a further investigation on mechanical properties, various tests for determining moisture content, optical properties, porosity, surface roughness, density, tensile strength, tensile energy absorption (TEA), stretch, stiffness, tear index, burst index, zero-span tensile strength, and internal bond strength were conducted at CPI.

Figures 1 to 5 shows some key results of the tests. The ideal combination of sack kraft pulp and BCTMP will be determined after comparing to the target need of the industry and the analysis will be reported in the future work.

Next steps

Additional testing at University of Toronto's Pulp and Paper Centre will involve applying coating to the handsheets to provide omniphobic properties, and improve oil and water barrier features. It is crucial to find suitable replacements to the commonly used fluorinated based coatings, as they have poor recyclability, low biodegradability, and are toxic. Any alternative must achieve the same liquid repellency while reducing toxicity and negative health impacts. Various experiments have already attempted to find an eco-friendly coating substitute for the FPP. The repellency of the new non-fluorinated coatings will be examined on the best combination of sack kraft pulp and BCTMP, and the outcomes of that research will be reported in another issue of this newsletter.

PUBLICATIONS, PAPERS AND CONFERENCES

We are pleased to announce titles of recent articles published in peer reviewed journals, and of some papers and presentations of our ERMP researchers.

Journal Articles

- Fernandez F., D.M. Martinez, and J.A. Olson. 2018. "Investigation of low consistency reject refining of mechanical pulp for energy savings." *Nordic Pulp and Paper Research Journal*. 33(1):17–22.
- Harirforoush R., J.A. Olson, P. Wild. 2018. "Indications of the onset of fiber cutting in low consistency refining using a refiner force sensor: the effect of pulp furnish." *Nordic Pulp and Paper Research Journal*. 33(1):48–57.
- Rubiano Berna J.E., D.M. Martinez, and J.A. Olson. 2018. "A comminution model parametrization for low consistency refining," *Powder Technology*. 328: 288–99.

Papers and Presentations at Conferences

- Olson J.A. 2018. "Review of Energy Reduction in Mechanical Pulping Research Program with emphasis on LC Refining." Presentation at *PaperWeek Canada Conference, February 8,* Montreal, Quebec, Canada.
- Harirforoush, R., J.A. Olson, and P. Wild. 2018. "The effect of recirculation mode on bar forces in low consistency refining." Presentation at *PACWEST Conference, May 30–June 2.* Jasper, Alberta, Canada.
- Kordi, T., S. Hossain, P. Bergström, R. Farnood, and T. Uesaka. "Discrete Element Modelling of Plybond Strength". 2018. Presentation at the *PACWEST Conference, May 30–June 2*. Jasper, Alberta, Canada.
- Tian H., and R.B. Gopaluni. "Moving Horizon Estimator Design for Mechanical Pulping Process". 2018. Presentation at the *PACWest Conference, May 20-June 2,* Jasper, AB, Canada.

Dissertation

- Harirforoush, R. 2018. *The Potential Use of Bar Force Sensor Measurements for Control in Low Consistency Refining.* Ph.D. Dissertation. University of Victoria, British Columbia, Canada. https://dspace.library.uvic.ca/handle/1828/9020.

TRIAL UPDATES

Over the winter of 2017 and spring of 2018, ERMP engaged in several LC refining projects outside the work of our graduate students. We have continued our collaboration with visiting researcher Hui Cai from Nanjing Forestry University, Jiangsu, China, adding several additional refining trials to her work on OCC (old corrugated cardboard). Our project with Meadow Lake continues with numerous fractionation and LC refining trials completed under a range of operating conditions and pulp types. We are working with Canfor Pulp Innovation to conduct large volume LC refining, and have collaborated with a university in Australia on a micro-fibrillated cellulose (MFC) project.

Last year's Andritz Trials were held at the Andritz R&D Center in Springfield, Ohio from December 18-21, 2017, with Meaghan Miller, James Olson, Jorge Rubiano, and Vanessa Van Aert in attendance. Our research collaborated with Millar Western, and studied the effect of low-consistency refining on reject Aspen pulp. The trial report for the latest Andritz project is currently under review, eventually to be circulated with our partners. Additionally, highly-refined TMP was created and combined with primary refined Aspen pulp to investigate the effects of adding MFC in lieu of a secondary LCR stage. SEM-image analysis of handsheets made of these composite samples is currently underway at the UBC Bio-imaging facility.

Left: The 22" TwinFLO double disc LC Refiner at Andritz R&D Center, Springfield used in ERMP's 2017 Andritz trials.

The UBC-PPC laboratory has recently benefited from the addition of new equipment. A compression tester arrived in January, which is currently fitted to perform a Ring Crush Test of paperboard, and is also capable of other testing such as the Edge Crush Test (ECT), Flat Crush Test (FCT) and Column Crush Test (CCT) to name a few.

The Dynamic Sheet Former (DSF) along with sheet dryer and press discussed last newsletter is expected to arrive in the spring of 2018, purchased with financial support from NSERC. The DSF will allow us to make single and multi-layered sheets similar to a commercial paper machine. The PPC laboratory is also in the planning phase of incorporating our MR8 fractionation screen into our LC refiner loop system and adding a new repulper tank donated by Canfor Pulp. Once completed the new configuration will enable us to become more efficient and effective in conducting fractionation and reject refining operations.

Left: Crush tester, purchased in January 2018.

Upcoming Event

The ERMP Steering Committee Meeting, usually held in June along with the PACWest Conference, has been deferred to early fall owing to a schedule overlap.

We will notify all ERMP Steering Committee members of the revised date and venue as soon as a decision is made.

ERMP PERSONNEL CHANGES

Farewells

We said goodbye to research technician Vanessa Van Aert in May, who is leaving UBC-PPC to pursue a new job opportunity on the East coast. Vanessa assisted in many LCR and MR8 pilot plant trials, and helped with the daily responsibilities of the laboratory, as well as being a part of the 2017 Andritz trials. Although she has thoroughly enjoyed her time working with the ERMP team, she is looking forward to her move to Eastern Canada where she will be partnered with a start-up company. We congratulate Vanessa, and wish her the best of luck to pursue a great career opportunity.

We also want to thank two of our departing Work-Learn students as they continue with their education. Jocelyn Zhou and Shayan Hosseinpour were both hard working students whose assistance ensured the smooth operation of our pilot plant and wet laboratory facilities. Jocelyn and Shayan contributed to numerous projects during their time with us and gained exposure to various pieces of equipment and procedures common to the pulp and paper industry.

Research technicians Vanessa and Reanna in the High Head lab, set up equipment prior to an LC refining trial. Work-Learn student Shayan, on the left, assists.

Welcoming new arrivals

This summer we will be welcoming two new undergraduate students to our team; Olivia Garland and Jwal Prajapati. Olivia is a Chemical and Biological Engineering major, and Jwal comes with an Electrical Engineering major. They joined our group to acquire practical hands-on laboratory-based experience, and gain an introduction to industry practices. Over the summer these students will be assisting with pilot-scale low consistency refining trials as well as pulp and paper testing.

Olivia and Jwal in the paper testing laboratory.

Meaghan Miller, ERMP Project Manager, is on parental leave into spring 2019. She delivered a healthy baby boy, Arlo, weighing 7 lb and 3 oz., on the Easter Sunday of April 1 at the BC Women and Children's Hospital, Vancouver.

Baby Arlo at two weeks.

CONTACTS

You are welcome to contact any of the faculty or staff:

Meaghan Miller*
Program Manager
604-827-2390
Meaghan.Miller@ubc.ca
* On maternity leave.

James Olson
Professor, UBC
604-822-2693
James.Olson@ubc.ca

Mark Martinez
Professor, UBC
604-822-2693
Mark.Martinez@ubc.ca

Rodger Beatson
Professor, BCIT
604-432-8951
Rodger_Beatson@bcit.ca

Peter Wild
Professor, UVic
250-721-8901
PWild@uvic.ca

Bhushan Gopaluni
Professor, UBC
604-827-5668
Bhushan.Gopaluni@ubc.ca

Boris Stoeber
Professor, UBC
604-827-5907
Boris.Stoeber@ubc.ca

Ramin Farnood
Professor, UofT
416-946-7525
Ramin.Farnood@utoronto.ca

Chitra Arcot
Communications Coordinator, UBC
604-827-2117
Chitra.Arcot@ubc.ca

www.EnergyReduction.ppc.ubc.ca

PARTNERSHIP IS OUR STRENGTH

The supporting partners of this research program are:

AB Enzymes, Alberta Newsprint Company, Andritz, BC Hydro, BCIT, Canfor, Catalyst Paper, FPInnovations, Holmen Paper, Meadow Lake Pulp, Millar Western, NORPAC, NSERC, The University of British Columbia Pulp and Paper Centre, The University of Victoria, The University of Toronto Pulp and Paper Centre, West Fraser, Westcan Engineering, and Winstone Pulp International.